Calculation of the ${}^4_\Sigma$He Bound State in the ^{4}He(K^-,π^-) Reaction at 600 MeV/c

Toru Harada

Department of Social Information, Sapporo Gakuin University, Ebetsu, Hokkaido 069-8555, Japan

(Received 28 August 1998)

We examine phenomenologically the ^{4}He(in-flight K^-,π^-) spectrum at $p_{K^-} = 600\,\mathrm{MeV}/c$ and $\theta_{K\pi} = 4°$ within distorted-wave impulse approximation calculations by using a coupled ($3N$-Λ) + ($3N$-Σ) model. The result shows that there exists a pole of the ${}^4_\Sigma$He unstable bound state on the second Riemann sheet of the complex energy plane, and its complex eigenvalue is $E^{(\mathrm{pole})}_{\Sigma^+} = -1.1 - i6.2$ MeV near the Σ threshold. Because of the Σ branch cut associated with opening the Σ channel, an asymmetric peak for ${}^4_\Sigma$He appears with lying at 3.7 MeV below the Σ^{+3}H threshold and the width of about 10 MeV, which is in good agreement with the recent observation. [S0031-9007(98)07879-X]

PACS numbers: 21.80.+a, 25.80.Pw, 27.10.+h

Recently, Nagae *et al.* [1] confirmed the existence of the ${}^4_\Sigma$He bound state in the in-flight ^{4}He(K^-,π^-) reaction at 600 MeV/c (4°) in the E905 experiments at BNL. This state might be interpreted as a strange partner of the α particle [2], together with the ${}^4_\Lambda$He ground state. Therefore, it is of great importance to understand the structure of the ${}^4_\Sigma$He bound state, which has $J^\pi = 0^+$ and $T \simeq \frac{1}{2}$, because the flavor SU(3) nature seems to survive in the Σ-hypernuclear side [3].

It has been discussed for about ten years whether ${}^4_\Sigma$He is a bound state or not. Hayano *et al.* [4] reported the first observation of the ${}^4_\Sigma$He bound state in the ^{4}He (stopped K^-,π^-) reaction at KEK. However, Dalitz and Deloff [5] suggested that the observed peak originates from a threshold cusp at the Σ^{+3}H threshold, reanalyzing the exclusive π^- data from the stopped K^- by helium bubble chambers (HeBC). Because the atomic orbit where K^- is absorbed on the K^--^{4}He atom is unknown, we could not refute their opinion only from the theoretical analysis of the ^{4}He (stopped $K^-,\pi^\mp$) data [6].

In contrast to the stopped K^- reactions, the in-flight K^- reaction enables us to choose the experimental condition; the recoil momentum for Σ (Λ) amounts to $q_\Sigma \simeq$ 120 MeV/c ($q_\Lambda \simeq 54$ MeV/c) at 600 MeV/c. The substitutional recoil-less condition on the ^{4}He target is suited to populate hypernuclear states with $J^\pi = 0^+$. Thus the E905 experiments realized that the peak of ${}^4_\Sigma$He is clearly observed below the Σ threshold, as shown in Fig. 1.

On the other hand, it has long been recognized that the ΛN-ΣN coupling plays a significant role in understanding the hypernuclear problems, see, e.g., Refs. [8,9]. The coupling is expected to be one of the key elements for solving the anomalous binding energies of ${}^4_\Lambda$He, ${}^4_\Lambda$H, and ${}^5_\Lambda$He [10,11]. Moreover, the strong $\Sigma N \to \Lambda N$ conversion causes a threshold cusp at the $\Sigma^+ p$ threshold in the $K^- d \to \pi^- \Lambda p$ reaction [12]. Consequently, we believe now that the $A = 4$ hypernuclei, ${}^4_\Lambda$He and ${}^4_\Sigma$He, are very promising objects to be studied in order to see the importance of the Λ-Σ coupling quantitatively.

In this Letter we examine phenomenologically the ^{4}He(K^-,π^-) spectrum with the distorted-wave impulse approximation (DWIA) by using a coupled ($3N$-Λ) + ($3N$-Σ) model, in order to establish the structure of the ${}^4_\Sigma$He bound state. Our purpose here is to determine the pole position of ${}^4_\Sigma$He from the experimental data and to demonstrate the spectrum behavior when its pole near the Σ threshold resides away from the physical region by the Σ branch cut.

Now we consider hypernuclear final states from the K^--^{4}He reaction classified as

$$\begin{aligned} K^- + {}^4\mathrm{He} \to\ &(a)\ \pi^- + {}^3\mathrm{He} + \Lambda\,,\\ &(b)\ \pi^- + {}^3\mathrm{H} + \Sigma^+,\\ &(c)\ \pi^- + {}^3\mathrm{He} + \Sigma^0,\\ &(d)\ \pi^- + X^{++} + \Lambda\,, \end{aligned} \tag{1}$$

where $X^{++} = d + p$ or $p + p + n$ for the π^- spectrum. It has been realized that an enhancement near the Σ^{+3}H threshold in the π^- spectrum of Eq. (1) is connected with the dominance of the secondary process,

$$[{}^4_\Sigma\mathrm{He}] \to X^{++} + \Lambda\,, \tag{2}$$

where the produced Σ hyperon in the real or virtual ${}^4_\Sigma$He state subsequently interacts with a second nucleon, and it is converted to a Λ via the internal $\Sigma N \to \Lambda N$ processes. The conversion induces generally the core-nuclear breakup because a converted ΛN pair gets large energy from the mass difference $m_\Sigma - m_\Lambda \simeq 80$ MeV. Indeed, the HeBC data suggest that $3N$ breakup states of (d) $\pi^- + X^{++} + \Lambda$ contribute dominantly near the Σ threshold rather than those of (a) $\pi^- + {}^3$He $+ \Lambda$ [5], while contributions of $3N$ breakup states in Σ channels are negligible. Quantum mechanically, the mechanism of the enhancement is associated with a pole for ${}^4_\Sigma$He in the s-wave scattering amplitude of Eq. (1). Such a pole resides on the *second* Riemann sheet ($-{+}{+}$) [13], which describes an *unstable* bound state in the Σ channel and gives rise to a resonance in the Λ channel. The pole position corresponds to a complex *eigenvalue* of the $3N$-Y

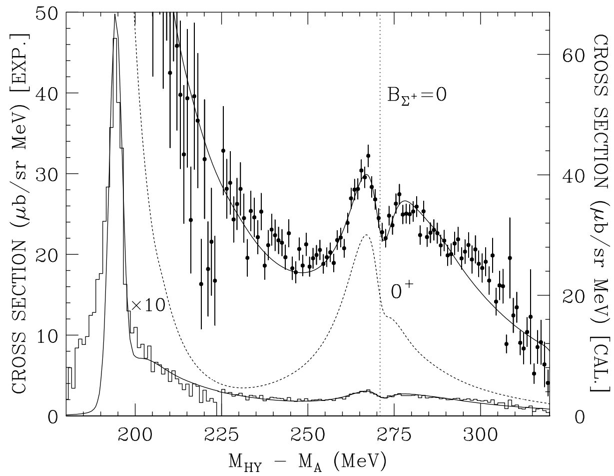

FIG. 1. The calculated spectrum of the ^{4}He(K^-, π^-) reaction at 600 MeV/c (4°), together with the BNL data [1], as a function of the hypernuclear energy $\Delta M_{\rm HY} = M_{\rm HY} - M_{\rm A}$. The histogram redraws the data to compare the spectrum with the data of the Λ region [7]. A peak at 194 MeV corresponds to the $^4_\Lambda$He ground state. The solid and dashed lines denote the π^- spectra for the total and $J^\pi = 0^+$ states, respectively, with a detector resolution of 3.63 MeV FWHM.

system on the complex energy plane. To establish the structure of a $^4_\Sigma$He bound state, it is necessary to extract its pole position from the observed spectrum.

The inclusive double-differential cross section for $(K^-, \pi^\mp)$ reactions in DWIA [6] is estimated by using the Green's function method [14]; the meson distorted waves are calculated with the help of the eikonal approximation. The Fermi-averaged amplitudes $\overline{f}_{(Y\pi)}$ for $K^-N \to \pi Y$ reactions are obtained from the free ones [15]. The hypernuclear final states with the natural parities, $0^+,\ 1^-,\ 2^+, \ldots,$ are considered because the spin-flip processes are known to be negligible in $(K^-, \pi^\mp)$ reactions at 600 MeV/c [15]. Our calculations have assumed that the $3N$ core nucleus is rigid, where $3N$ denotes the (^{3}He, ^{3}H) doublet. Thus Green's function of the $3N$-Y final states in Eq. (1) is obtained by solving a coupled equation with ^{3}He + Λ, ^{3}H + Σ^+, and ^{3}He + Σ^0 channels. The $3N$-Y potential matrix with $J^\pi = 0^+$ on the isospin bases is given by

$$\hat{U} = \begin{pmatrix} U_{\Lambda,1/2} & U_{X,1/2} & 0 \\ U_{X,1/2} & U_{\Sigma,1/2} & 0 \\ 0 & 0 & U_{\Sigma,3/2} \end{pmatrix}. \tag{3}$$

The diagonal potentials for $T = \frac{1}{2},\ \frac{3}{2}$ are given as

$$U_{Y,T}(R) = V_{Y,T}(R) + iW_{Y,T}(R) \tag{4}$$

for $Y = \Sigma,\ \Lambda$, where the imaginary part $W_{Y,T}$ is a spreading potential, which describes effectively all of the $3N$ breakup processes. The Λ-Σ coupling potential $U_{X,1/2}$ is assumed to be real. We obtain these potential forms by folding the central YN interaction like SAP-1 [16] with the core-nuclear $3N$ density. Therefore, the diagonal potentials have a repulsive core and an attractive tail, of which strengths can be determined to fit the experimental data.

In our framework, we search for parameters of potential strength $U_{\Lambda,1/2}$, $U_{X,1/2}$, $U_{\Sigma,1/2}$, and $U_{\Sigma,3/2}$ by making a fit to the experimental data. Since the ^{4}He(K^-, π^+) reaction populates only $T = \frac{3}{2}\ \Sigma$ states, we determine $U_{\Sigma,3/2}$ by fitting the π^+ data. The $3N$-Y system has a bound state with $J^\pi = 0^+$ in the Λ channel, which is the $^4_\Lambda$He ground state with $B_\Lambda = 2.39$ MeV. Thus we put a constraint on the parameters to fit this value. For given $U_{X,1/2}$, we can determine a set of $V_{\Lambda,1/2}$ and $V_{\Sigma,1/2}$. Here we made $U_{X,1/2}$ satisfy a plausible Σ admixture of about 2% in $^4_\Lambda$He [17]. In addition, the Fermi-averaged amplitudes $\overline{f}_{(Y\pi)}$ remain in ambiguities, so the relative phase of φ_Λ (φ_Σ) for $\Lambda\pi$ ($\Sigma\pi\ I = 1$) to $\Sigma\pi\ I = 0$ channels should be determined from the present fit [18].

The five parameters of the strengths ($V_{\Lambda,1/2}$, $V_{\Sigma,1/2}$, $W_{\Sigma,1/2}$) and the phases ($\varphi_\Lambda, \varphi_\Sigma$) are determined by fitting the π^- data overall; $V_{\Lambda,1/2}$ and $V_{\Sigma,1/2}$ are well determined by the existence of two peaks for $^4_\Lambda$He and $^4_\Sigma$He in the data. To make a detailed fit to the shape near the Σ threshold, we tune $W_{\Sigma,1/2}$, φ_Λ, and φ_Σ. As a result, we obtain the $3N$-Y potential for the best fit. Using the potential, we can also explain the data of HeBC [5] and ^{4}He (stopped K^-, $\pi^\mp$) [19] experiments.

Figure 2 displays the calculated ^{4}He(K^-, π^+) spectrum at 600 MeV/c (4°), together with the BNL data. We find that the calculated shape is in good agreement with the experimental one. The reduced χ^2-fitting value is $\chi^2/N = 12.7/31 = 0.41$ for $\Delta M_{\rm HY} = 270$–300 MeV. Therefore, we confirm that there is no bound state in $T = \frac{3}{2}$ for the ^{3}H + Σ^- channel, because the nucleus-Σ potential for $T = \frac{3}{2}$ is repulsive [6], which is quite similar to the potential derived from SAP-1 [16]. Some discrepancy of the absolute cross section might be improved by employing more realistic meson-distorted waves or refined amplitudes $\overline{f}_{(Y\pi)}$.

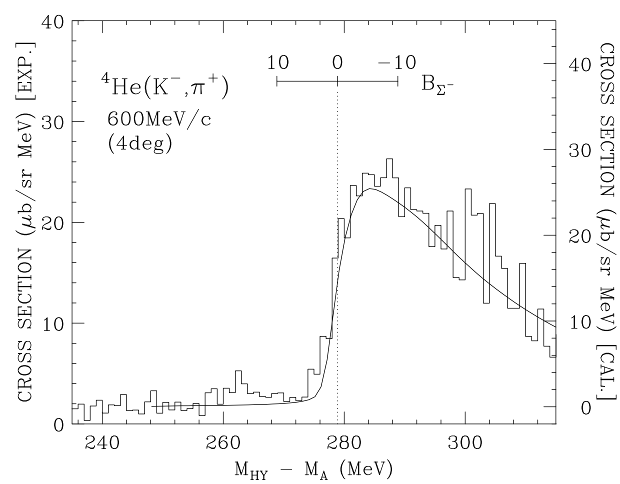

FIG. 2. The calculated spectrum of the ^{4}He(K^-, π^+) reaction at 600 MeV/c (4°), together with the BNL data [1].

For the ^{4}He(K^-,π^-) spectrum, as seen in Fig. 1, our $3N-Y$ calculation can qualitatively fit the data overall. We find that the meson-distorted effects are very important to reproduce the data. If we replace distorted waves by plane ones, the spectrum is too small to explain the data of $\Delta M_{\rm HY} = 220$–250 MeV region. Most important is the fact that the calculated curve can excellently fit to the peak behavior of the π^- spectrum near the Σ threshold [$\chi^2/N = 30.4/31 = 0.98$ for $\Delta M_{HY} = 250$–280 MeV].

The potential we determined shows us properties of the $3N$-Y system. In the $^4_\Lambda$He ground state, the Λ-Σ coupling leads to the Σ^+ (Σ^0) admixture of 1.30% (0.63%). When the coupling is turned off, the binding energy is obtained to be $B_\Lambda = 1.17$ MeV. We confirm that the Λ-Σ coupling is significant in $^4_\Lambda$He, which makes the binding energy increase by about 1.22 MeV. To obtain the pole position of $^4_\Sigma$He, we calculate the complex eigenvalue of the Hamiltonian for the $3N$-Y system by the complex scaling treatment. We find that there appears a pole of an *unstable* bound state with $J^\pi = 0^+$ in the Σ channel on the *second* Riemann sheet $(-++)$. This complex eigenvalue represents

$$E_{\Sigma^+}^{(\rm pole)} = (k_{\Sigma^+}^{(\rm pole)})^2/2\mu = -1.1 - i6.2 \text{ MeV}, \qquad (5)$$

where μ is the reduced mass of the ^{3}H + Σ^+ system and the real part of $E_{\Sigma^+}^{(\rm pole)}$ is measured from this threshold. The nature of the state originates from a strong isospin dependence of the Lane term in the $3N$-Y potential. We have confirmed that this Lane term plays an essential role in making the $3N$-Y system bound in the Σ channel and recovers the isospin symmetry to $T \simeq \frac{1}{2}$ (99%) [16]. However, since the pole resides near the Σ^{+3}H threshold, it is necessary to investigate Σ threshold effects on the spectrum shape.

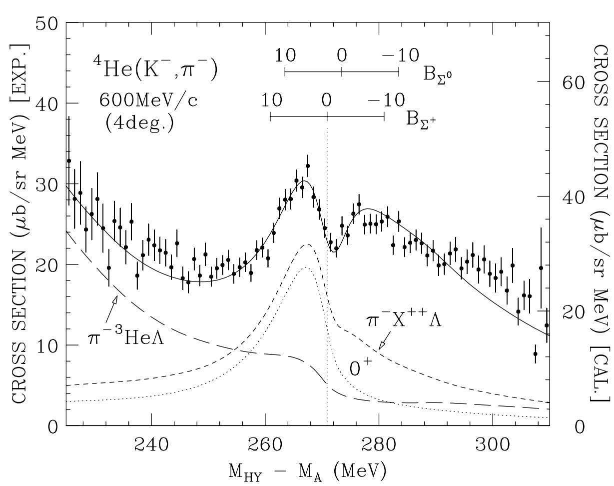

FIG. 3. Contributions to the ^{4}He(K^-,π^-) spectrum near the Σ threshold. The solid, long-dashed, and dashed curves are for the total π^-, π^- + ^{3}He + Λ, and π^- + X^{++} + Λ final states, respectively. The dotted curve denotes the contribution of $J^\pi = 0^+$ in the π^- + X^{++} + Λ final state.

Employing Green's function, we can easily estimate the contribution of each channel in Eq. (1) for the π^- spectrum [20]. Figure 3 illustrates the contributions of the Λ-emitted final states, (a) π^- + ^{3}He + Λ and (d) π^- + X^{++} + Λ, near the Σ threshold. In the spectrum of (a), a *rounded step* is observed at the Σ^{+3}H threshold. In the spectrum of (d), as we expected, there appears dominantly the peak of the $^4_\Sigma$He bound state; the produced $^4_\Sigma$He state spreads to the complicated Λ channels with core-nuclear breakup, which are described by $W_{Y,1/2}$ [20]. The calculated shape for $J^\pi = 0^+$ is clearly *asymmetric*, and its integrated cross section is about 220 μb/sr. This value is almost consistent with that reported by Nagae *et al.* [1], considering the large systematic error in their fitting.

To investigate how the shape of the π^- spectrum changes as the pole moves on the $(-++)$ sheet, we vary the strengths of the Λ-Σ coupling $U_{X,1/2}$ and of the spreading potential $W_{Y,T}$. In Fig. 4(b) we illustrate the resultant pole positions of the $3N$-Y system near the Σ threshold: We know the pole position of $^4_\Sigma$He to be at point D $(-1.1, -6.2)$ in a complex energy plane, as listed in Table I. When $U_{X,1/2}$ and $W_{Y,T}$ are turned off, this pole moves to point A $(-8.1, 0.0)$, which becomes

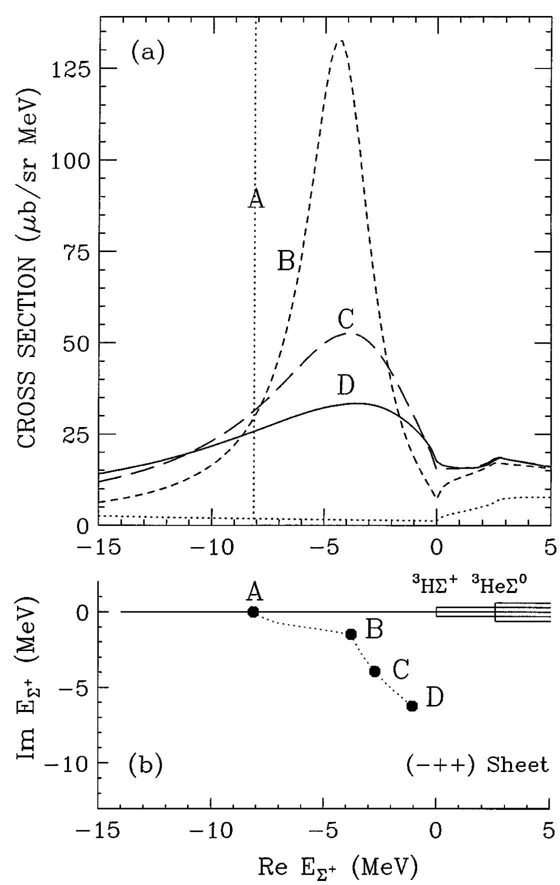

FIG. 4. (a) Behavior of the spectrum for $J^\pi = 0^+$ near the Σ threshold in the ^{4}He(K^-,π^-) reaction at 600 MeV/c (4°). (b) Behavior of the pole position for $^4_\Sigma$He on the $(-++)$ sheet. The labels A, B, C, and D are for each position given in Table I.

TABLE I. Positions of the poles of the $3N$-Y system near the Σ threshold in complex energy plane and complex momentum plane. The real part of the energy is measured from the Σ^{+3}H threshold. The case D is the best fit to the data.

	Sheet[a]	$E_{\Sigma^+}^{(\mathrm{pole})}$[b] (MeV)	$k_{\Sigma^+}^{(\mathrm{pole})}$[c] ($\mathrm{fm}^{-1}$)	$E_{\Sigma^+}^{(\mathrm{obs})}$[d] (MeV)
A	$(-++)$	-8.1	$+i0.591$	-8.1
B	$(-++)$	$-3.8 - i1.5$	$-0.077 + i0.411$	-3.9
C	$(-++)$	$-2.7 - i3.9$	$-0.210 + i0.402$	-3.8
D	$(-++)$	$-1.1 - i6.2$	$-0.335 + i0.399$	-3.7

[a]The sheets are identified by the signs of $(\mathrm{Im}\, k_\Lambda, \mathrm{Im}\, k_{\Sigma^+}, \mathrm{Im}\, k_{\Sigma^0})$.
[b]Pole position in the complex energy plane; $E_{\Sigma^+}^{(\mathrm{pole})} = (k_{\Sigma^+}^{(\mathrm{pole})})^2/2\mu$, where μ is the reduced mass of the ^{3}H + Σ^+ system.
[c]Pole position in the complex momentum plane.
[d]Observed energy $E_{\Sigma^+}^{(\mathrm{obs})} = -|\mathrm{Im}\, k_{\Sigma^+}^{(\mathrm{pole})}|^2/2\mu$.

the $3N + \Sigma$ bound state with $B_{\Sigma^+} = 8.1$ MeV. After only $U_{X,1/2}$ is turned on do we introduce a parameter R in the spreading potential, $R \times W_{Y,T}$, and consider values of $R = 0.0$, 0.5, and 1.0. As shown in Fig. 4, we can pass to points B, C, and D, and obtain the $J^\pi = 0^+$ spectra corresponding to positions of these poles. We find that the shape of the spectrum B is almost symmetric, as its pole lies near the physical axis. On the contrary, when the spreading potential increases, the peak structure of the spectrum is quite distorted and the cross section is reduced. The spectrum D falls rapidly above the Σ threshold and gives us the asymmetric width of about 10 MeV. In our calculation, therefore, the spreading potential is significant to reproduce the asymmetric shape and absolute value of the peak in the experimental data. This is because the pole on the $(-++)$ sheet is shadowed from physical view by the Σ branch cut opening at the Σ threshold. In such a case, the position of the peak in the spectrum does not necessarily correspond to the real part of the complex eigenvalue of $E_{\Sigma^+}^{(\mathrm{pole})}$ [21].

In order to understand this situation, it is suitable to consider the complex momentum plane with a cut on the real axis starting at the Σ threshold momentum. In topological consideration, the position of the peak in the spectrum might correspond to the observed energy $E_{\Sigma^+}^{(\mathrm{obs})} = -|\mathrm{Im}\, k_{\Sigma^+}^{(\mathrm{pole})}|^2/2\mu$. This energy is for the foot of the perpendicular from the pole of $^4_\Sigma$He to the imaginary axis in the complex momentum plane, and it gives the minimum distance between the pole and the physical axis. The values of $E_{\Sigma^+}^{(\mathrm{obs})}$ given in Table I are in good agreement with the peak positions in the asymmetric spectra drawn in Fig. 4(a). Therefore, we can recognize the asymmetric spectrum for $^4_\Sigma$He, of which the peak lies at 3.7 MeV below the Σ^{+3}H threshold and its width is about 10 MeV. These values should be compared with experimental ones reported by Nagae *et al.* $B_{\Sigma^+} = 4.4 \pm 0.3 \pm 1$ MeV and $\Gamma = 7.0 \pm 0.7^{+1.2}_{-0.0}$ MeV [1], and by Outa *et al.* $B_{\Sigma^+} = 2.8 \pm 0.7$ MeV and $\Gamma = 12.1 \pm 1.2$ MeV [19].

In summary, we have examined phenomenologically the ^{4}He(K^-, π^-) spectrum at 600 MeV/c by using the coupled-channel framework between the ^{3}He + Λ, ^{3}H + Σ^+, and ^{3}He + Σ^0 channels with a spreading potential. Our result shows that a pole of the $^4_\Sigma$He unstable bound state with $J^\pi = 0^+$ and $T \simeq \frac{1}{2}$ (99%) is located at $E_{\Sigma^+}^{(\mathrm{pole})} = -1.1 - i6.2$ MeV on the second Riemann sheet $(-++)$. Because of the Σ threshold effect, the asymmetric peak appears with lying at 3.7 MeV below the Σ^{+3}H threshold and the width of about 10 MeV. We believe that the present study gives us a starting point to unified hypernuclear studies from Λ to Σ regions.

The author thanks Professor Y. Akaishi, Professor T. Nagae, Professor R. Sawafta, Mr. H. Outa, Dr. Y. Shimizu, and Dr. Y. Hirabayashi for many valuable discussions. This work was supported by the Grants-in-Aid for Scientific Research of the Japanese Ministry of Education, No. 08239104.

[1] T. Nagae *et al.*, Phys. Rev. Lett. **80**, 1605 (1998).
[2] T. Harada, Nucl. Phys. **A547**, 165c (1992).
[3] T. Harada, Few-Body Syst. Suppl. **9**, 155 (1995).
[4] R. S. Hayano *et al.*, Phys. Lett. B **231**, 355 (1989).
[5] R. H. Dalitz and A. Deloff, Nucl. Phys. **A547**, 181c (1992); **A585**, 303c (1995), and references therein.
[6] T. Harada and Y. Akaishi, Prog. Theor. Phys. **96**, 145 (1996).
[7] T. Nagae (private communication).
[8] Y. Nogami and E. Satoh, Nucl. Phys. **B19**, 93 (1970).
[9] B. F. Gibson *et al.*, Prog. Theor. Phys. Suppl. **117**, 339 (1994), and references therein.
[10] B. F. Gibson *et al.*, Phys. Rev. C **6**, 741 (1972).
[11] J. Dabrowski, Phys. Rev. C **8**, 835 (1973).
[12] R. H. Dalitz, Nucl. Phys. **A354**, 101c (1981), and references therein.
[13] The sheet is identified by three signs of $(\mathrm{Im}\, k_\Lambda, \mathrm{Im}\, k_{\Sigma^+}, \mathrm{Im}\, k_{\Sigma^0})$, where k_Y denotes the c.m. momentum of the $3N$-Y system in the complex momentum plane.
[14] O. Morimatsu and K. Yazaki, Nucl. Phys. **A483**, 493 (1988).
[15] G. P. Gopal *et al.*, Nucl. Phys. **B119**, 362 (1977).
[16] T. Harada *et al.*, Soryushiron Kenkyu **76**, 25 (1987); Nucl. Phys. **A507**, 715 (1990).
[17] Y. Akaishi, T. Harada, and S. Shinmura (to be published).
[18] R. H. Dalitz and A. Deloff, Czech. J. Phys. B **32**, 1021 (1982).
[19] H. Outa *et al.*, Prog. Theor. Phys. Suppl. **117**, 171 (1994).
[20] T. Udagawa *et al.*, Phys. Rev. C **49**, 3162 (1994).
[21] I. R. Afnan and B. F. Gibson, Phys. Rev. C **47**, 1000 (1993).